

# The 21-cm Signal from the Cosmological Epoch of Recombination

A. Fialkov<sup>a,c</sup> and A. Loeb<sup>b,c</sup>

<sup>a</sup>Departement de Physique, Ecole Normale Supérieure, CNRS,  
24 rue Lhomond, 75005 Paris, France

<sup>b</sup>Department of Astronomy, Harvard University,  
60 Garden Street, MS-51, Cambridge, MA, 02138, USA

<sup>c</sup>The Raymond and Beverly Sackler School of Physics and Astronomy, Tel Aviv University,  
Tel Aviv 69978, Israel

E-mail: [anastasia.fialkov@phys.ens.fr](mailto:anastasia.fialkov@phys.ens.fr); [aloeb@cfa.harvard.edu](mailto:aloeb@cfa.harvard.edu)

**Abstract.** The redshifted 21-cm emission by neutral hydrogen offers a unique tool for mapping structure formation in the early universe in three dimensions. Here we provide the first detailed calculation of the 21-cm emission signal during and after the epoch of hydrogen recombination in the redshift range of  $z \sim 500-1, 100$ , corresponding to observed wavelengths of 100–230 meters. The 21-cm line deviates from thermal equilibrium with the cosmic microwave background (CMB) due to the excess Ly $\alpha$  radiation from hydrogen and helium recombinations. The resulting 21-cm signal reaches a brightness temperature of a milli-Kelvin, orders of magnitude larger than previously estimated. Its detection by a future lunar or space-based observatory could improve dramatically the statistical constraints on the cosmological initial conditions compared to existing two-dimensional maps of the CMB anisotropies.

---

## Contents

<b>1</b>	<b>Introduction</b>	<b>1</b>
<b>2</b>	<b>21-cm signal from <math>z &gt; 500</math></b>	<b>2</b>
2.1	The Ly $\alpha$ background	2
2.2	Results	4
<b>3</b>	<b>Conclusions</b>	<b>8</b>

---

## 1 Introduction

Hydrogen atoms provide an excellent tracer for the evolution of structure from the epoch of recombination at  $z \sim 1,100$ , when these atoms first formed, to the epoch of reionization at  $z \sim 7$ , when they were broken to their constituent electrons and protons [1]. The 21-cm transition between the two hyperfine levels of the 1S ground state has a small optical depth, and so the signal from each redshift  $z$  can be mapped independently by measuring the extra-Galactic emission at redshifted wavelengths of  $21 \times (1 + z)$  cm [2, 3]. Since the 21-cm signal is coupled to astrophysical sources and cosmological parameters at the emission redshift, it is expected to provide precious information about the conditions in the early Universe.

A major effort is currently underway to detect the 21-cm signal from the epoch of reionization in the redshift range of  $6 < z < 15$  corresponding to observed wavelengths of  $\sim 1.5$ –7 meters. The newly constructed arrays of radio dipole antennae include the Murchison Widefield Array (MWA) [4], the LOw Frequency ARray (LOFAR) [5], the Precision Array for Probing the Epoch of Reionization (PAPER) [6], and the Large Aperture Experiment to Detect the Dark Ages (LEDA) [7], and plans exist for the next generation experiments that may reach up to  $z \sim 30$ , such as the Hydrogen Epoch of Reionization Array (HERA)<sup>1</sup> the Square Kilometer Array (SKA) [8] and the Dark Ages Radio Explorer (DARE) [9].

The primary challenge for detecting the redshifted 21-cm signal involves the foregrounds of Galactic and extragalactic synchrotron emission which brightens with decreasing photon frequency. The foreground emission at very low frequencies is poorly constrained, and in fact, there are no available maps of all-sky emission at frequencies below 30 MHz. The state of the art in this field are maps of a part of the southern sky at resolution of  $5^\circ$ – $30^\circ$  measured from the ground [10] and maps produced by the Radio Astronomy Explorer-2 satellite with the resolution of  $> 30^\circ$  made in the 1970s [11]. Only few space-based observations were conducted so far in the frequency range 1–20 MHz, where the electrons in the ionosphere block our ground-based view of the universe [12–14]. Naturally, a space or moon-based low-frequency radio array would not suffer from the drawbacks of the Earth’s ionosphere, as well as from the interference noise introduced by terrestrial radio and TV stations. A number of experiments have been proposed to measure the cosmic radiation at the long wavelengths, which includes a network of freely flying spacecrafts working as an antenna array [15], and an antenna array installed on the moon

---

<sup>1</sup><http://reionization.org/>

[16, 17]. Such arrays would not suffer from ionospheric distortions or from the radio-frequency interference and would be able to access Galactic and extragalactic hectometer emission, i.e. the wavelength regime corresponding to the range at which the redshifted 21-cm signal all the way to the epoch of recombination at  $z \sim 10^3$  may be found.

The 21-cm signal of neutral hydrogen from the dark ages prior to star formation [18, 19] is expected to be extremely weak and particularly challenging to observe. Here we revisit previous calculations and include for the first time the effect of the UV radiation that builds up during the cosmic recombination epoch of hydrogen. In particular, the excess photons near the Ly $\alpha$  resonance are immediately reabsorbed by neutral hydrogen atoms, driving the 21-cm transition out from thermal equilibrium with the cosmic microwave background (CMB). The associated Wouthuyson-Field (WF) effect [20, 21] couples the 21-cm emission (or absorption) to the color temperature of the Ly $\alpha$  field, boosts the magnitude of the 21-cm signal from  $z > 500$  and improves its prospects for a future detection.

Our study has become possible due to recent advances in calculating the spectral distortions of the CMB during the cosmic recombination epoch. Two independent codes, HyRec [22] and CosmoRec [23], were developed to accurately solve the atomic physics together with the spectral distortions of the UV background around Lyman-series resonances. The two codes work in a similar manner by implementing an efficient and accurate method for solving the multi-level atom recombination problem [24], which accounts for an large number of excited states. The codes include all important processes that affect the recombination history, such as two-photon transitions (emission, absorption, Raman scattering) from the 2s hydrogen state and from higher levels, and frequency diffusion in the Ly $\alpha$  line, but they ignore collisional transitions. The main difference between the two codes from our perspective is that CosmoRec accounts for the effect of helium on the recombination radiation, while HyRec only includes the contribution from hydrogen. The photons emitted during helium recombination at  $z \sim 2500$ , contribute to the intensity of the radiative background near the Ly $\alpha$  resonance at the lower redshifts considered here [25] and therefore play a role in the WF effect. We therefore choose to use the output spectral distortions from CosmoRec for this work.

The paper is organized as follows. In §2 we discuss the UV background during and shortly after recombination and show the effect of this background on the 21-cm signal from this epoch, in §3 we remark on future observations of the hectometer signal and conclude. Throughout our discussion we adopt the standard set of cosmological parameters:  $h = 0.6704$ ,  $\Omega_c h^2 = 0.1204$ ,  $\Omega_b h^2 = 0.0220$ ,  $\Omega_\Lambda = 0.6817$ ,  $Y_P = 0.2477$ ,  $n_s = 0.9619$ ,  $\ln(10^{10} A_s) = 3.098$ ,  $k_0 = 0.05 \text{ Mpc}^{-1}$  [26]. As mentioned we use CosmoRec, available online<sup>2</sup>, in our calculations of the 21-cm signal.

## 2 21-cm signal from $z > 500$

### 2.1 The Ly $\alpha$ background

For a fixed set of cosmological parameters, the neutral hydrogen emission at high redshifts prior to cosmic star formation is fully determined by atomic physics. The key processes that determine the expected signal from this epoch are: (i) the WF effect of the Ly $\alpha$  photons from recombination; (ii) the coupling to the CMB, which tends to bring the hydrogen atoms to equilibrium with

---

<sup>2</sup>[www.chluba.de/cosmorec](http://www.chluba.de/cosmorec)

the thermal bath of the CMB photons at the temperature  $T_{CMB}$ ; and (iii) collisions. The effect of collisions on the 21-cm signal from dark ages is well understood [18, 19]. The neutral hydrogen emission from redshifts higher than  $z \sim 50$ , which in the standard cosmological model marks the epoch when stars appeared for the first time [28], is completely decoupled from complex processes associated with star formation such as gas cooling, feedback of stellar radiation and metal enrichment, X-ray heating of the intergalactic medium, and Ly $\alpha$  feedback, which must be taken into consideration when making predictions for the 21-cm signal from lower redshifts [1]. At redshifts  $50 \lesssim z \lesssim 300$  collisions break the coupling of the 21-cm signal to the CMB and tend to redistribute the population of the excited,  $n_1$ , and ground,  $n_0$ , hyperfine states of the 1s hydrogen level in accordance with the Boltzmann factor  $(g_1/g_0) \exp(-T_*/T_K)$ , where  $T_K$  is the kinetic temperature of the gas (which at  $z > 300$  is very close to the CMB temperature),  $(g_1/g_0) = 3$  being the ratio of the spin degeneracy of the two (triplet and singlet) levels, and  $T_* = 0.068$  K the temperature corresponding to the energy difference between the two hyperfine levels. This signal, considered in references [18, 19], is determined by the atomic physics during the early stage of the evolution of the Universe and depends on the density of neutral hydrogen atoms, and their collision rates with other atoms, electrons and protons, which can be found in tabular form in the references [3], [29] and [30] for the hydrogen-hydrogen (H-H), hydrogen-electron (H-e) and hydrogen-proton (H-p) collisions respectively.

At yet higher redshifts, which are accurately considered in this paper for the first time, the Ly $\alpha$  background, produced during hydrogen recombination, plays a significant role. Understanding the Ly $\alpha$  background is essential when making realistic predictions for the redshifted 21-cm signal. The Ly $\alpha$  photons are absorbed and then re-emitted by hydrogen atoms. As a result of this process an atom may relax to a different hyperfine state than the initial one, and the number densities of atoms in excited and ground hyperfine states are redistributed, through the WF effect. If the WF effect dominates the level distribution, the ratio of the number densities of the excited and the ground hyperfine states would be  $n_1/n_0 = 3 \exp(-T_*/T_C)$ , with  $T_C$  the color temperature of the Ly $\alpha$  photons defined via  $T_C^{-1} \equiv -\frac{k_B}{h_{pl}} \frac{d \ln n_\nu}{d\nu}$ , where  $k_B$  is the Boltzmann constant,  $h_{pl}$  is the Planck constant,  $\nu$  is the photon frequency and  $n_\nu = c^2 J_\nu / 2\nu^2$  is the photon occupation number with  $J_\nu$  being the intensity of the radiation field around the Ly $\alpha$  resonance (see Ref. [3] for more details). On the other hand, when the coupling  $x_\alpha$  of the Ly $\alpha$  field to the 21-cm line is weak, other processes determine the emission signal. The coupling is defined as

$$x_\alpha = \frac{4P_\alpha}{27A_{10}} \frac{T_*}{T_{CMB}}, \quad (2.1)$$

where  $P_\alpha = 4\pi\sigma_0 \int d\nu J(\nu)\phi_\alpha(\nu)$  is the total scattering rate of Ly $\alpha$  photons, with  $\phi_\alpha(\nu)$  the normalized Voigt profile,  $\sigma_0 = (\pi e^2/m_e c) f_\alpha$  [cm<sup>2</sup> s<sup>-1</sup>] and  $f_\alpha = 0.4875$  being the oscillator strength, and  $A_{10} = 2.85 \times 10^{-15}$  [s<sup>-1</sup>] is the spontaneous decay rate of the 21-cm line. Since  $x_\alpha$  depends on  $J_\nu$ , the resulting 21-cm signal is dictated by the intensity and color temperature of the radiation background around the Ly $\alpha$  resonance.

To find the intensity and the color temperature of the Ly $\alpha$  radiation at every instant one needs to accurately solve the recombination problem accounting for coupled evolution of level population of hydrogen and helium atoms and the UV radiation field, during hydrogen and helium recombination. Here we use the results of CosmoRec [23], which takes account of the important processes during cosmic recombination (but ignores the effect of collisions on the

level population). The radiative transfer of the Ly $\alpha$  photons is affected by: *(i)* emission and absorption that are not part of scattering processes; *(ii)* Hubble expansion, which shifts photons to lower frequencies; *(iii)* resonant scattering of the photons off of hydrogen atoms, which leads to energy exchange between photons and matter preserving the number of photons; and *(iv)* the 2s $\rightarrow$ 1s two-photon decay (see Ref. [27] for details). The optical depth for the Ly $\alpha$  photons during recombination is very high; when a hydrogen atom recombines and emits a Ly $\alpha$  photon, the photon is almost immediately reabsorbed by another hydrogen atom. Because of the large difference between the 2p $\rightarrow$ 1s transition rate and the Hubble rate, each photon close to the Ly $\alpha$  resonance scatters  $10^8 - 10^9$  times before it can escape, finally allowing a hydrogen atom to settle into the ground state. This process is known to create a bottleneck for recombination, but it also feeds the intensity of the radiation field around the Ly $\alpha$  resonance and thus the 21-cm signal from this epoch. The bottleneck for recombination is broken due to two main processes, the redshifting of the photons out of the Ly $\alpha$  resonance and the two-photon decay [31]. As recombination proceeds, additional atoms recombine to the ground state and the intensity of the radiation around the Ly $\alpha$  resonance declines.

The left panel of Figure 1 shows the redshift evolution of the intensity of the radiation background  $J_\nu$  (in units  $\text{s}^{-1}\text{cm}^{-2}\text{Hz}^{-1}\text{sr}^{-1}$ ) around the Ly $\alpha$  resonance. This intensity grows monotonically with increasing lookback time during hydrogen recombination, but is expected to decline after the epoch of helium recombination (HeII $\rightarrow$ HeI) at  $z \sim 2500$ . This Ly $\alpha$  background was our main motivation to consider the 21-cm signal from redshifts higher than the standard upper limit considered in the literature (e.g.,  $z \sim 300$  in [19]). The right panel of Figure 1 shows the spectral shape of the intensity in the vicinity of the Ly $\alpha$  resonance and the line profile (assumed to be the normalized Voigt profile) which are needed for the computation of  $x_\alpha$  in Equation (2.1).

## 2.2 Results

The deviation of the brightness temperature of the 21-cm signal from that of the CMB, is given by

$$T_b(z) = (1 - e^{-\tau}) \frac{(T_S - T_{CMB})}{(1+z)}, \quad (2.2)$$

where  $\tau$  is the optical depth for the 21-cm photons, and  $T_S$  is the spin temperature defined by the ratio between the density of atoms in the upper and lower states of the transition ( $n_1/n_0 = 3 \exp(-T_\star/T_S)$ ). To determine the spin temperature and make predictions for the observable brightness temperature, one should in principle evolve the number densities in time taking account of the Hubble expansion rate, the radiative transition rates due to the interaction with the CMB, the collisional spin excitation and de-excitation rates, and spin excitation and de-excitation rates from Ly $\alpha$  absorption [18]. However, at the redshifts of interest, the Hubble rate is sub-dominant compared to the other rates. As a result, we can safely assume that the system reaches a radiative equilibrium, in which case the spin temperature is given by [3]

$$\frac{1}{T_s} = \frac{T_{CMB}^{-1} + x_C T_K^{-1} + x_\alpha T_C^{-1}}{1 + x_C + x_\alpha}, \quad (2.3)$$

where  $x_C$  is the collisional coupling.

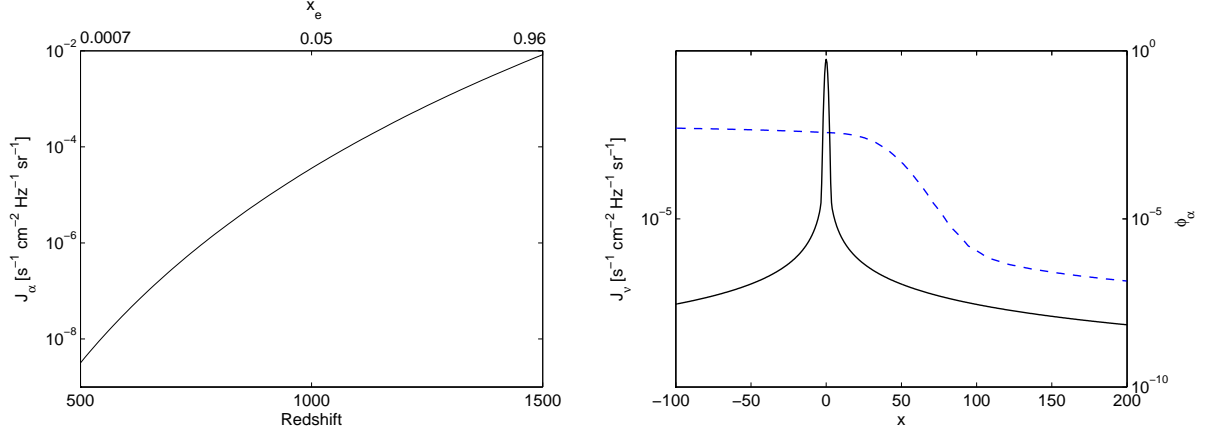


**Figure 1.** *Left:* Intensity of the radiation background  $J_\nu$  [ $\text{s}^{-1} \text{cm}^{-2} \text{Hz}^{-1} \text{sr}^{-1}$ ] at the Ly $\alpha$  resonance,  $\nu = \nu_\alpha$ , during hydrogen recombination (compiled using the CosmoRec code) as a function of redshift (lower horizontal axis) and the ionization fraction  $x_e$  (upper horizontal axis). *Right:* Spectral shape of  $J_\nu$  [ $\text{s}^{-1} \text{cm}^{-2} \text{Hz}^{-1} \text{sr}^{-1}$ ] around the Ly $\alpha$  resonance (dashed blue line, left axis) and the normalized Voigt profile of the Ly $\alpha$  line,  $\phi_\alpha$  at  $z = 1000$  (solid black line, right axis) as a function of  $x \equiv \frac{(\nu - \nu_\alpha)}{\nu_\alpha} \left( \frac{2k_B T_K}{m_H c^2} \right)^{-1/2}$ , where  $m_H$  is the hydrogen atom mass.

The dominant contribution to the brightness temperature of the 21-cm signal in the redshift range  $40 \lesssim z \lesssim 850$  originates from the collisional coupling. At higher redshifts this contribution alone vanishes due to the thermal coupling between the gas temperature and the CMB. However, when the effect of the early Ly $\alpha$  photons is added, at high redshifts the spin temperature couples to the color temperature of Ly $\alpha$ . On the left panel of Figure 2 we compare between the factor  $(1 - T_S/T_{CMB})$ , which contributes to the brightness temperature, and its limits at low redshifts  $(1 - T_K/T_{CMB})$  (the case of saturated collisional coupling) and at high redshifts  $(1 - T_C/T_{CMB})$  (the case of saturated WF coupling). The rapid evolution of the color temperature, shown on the Figure, reflects the fact that the slope of the radiation field around the Ly $\alpha$  resonance depends strongly on redshift and is determined by the aspects of atomic physics during hydrogen and helium recombination in addition to the cosmic expansion. The right panel of Figure 2 shows the relative importance of  $x_\alpha$  and  $x_C$  as a function of redshift. As is evident, collisional coupling dominates at redshifts below  $z \sim 850$  while  $x_\alpha$  dominates at higher redshifts. Thus, it is essential to account for the early WF effect when making predictions for the 21-cm signal from the epoch of recombination.

The global spectrum of neutral hydrogen, representing the average 21-cm brightness across the sky, is shown on the left panel of Figure 3. Its shape reflects the combined effects of collisional coupling and Ly $\alpha$  photons in addition to the radiative coupling to the CMB. The presence of the early Ly $\alpha$  photons leads to an enhancement in the 21-cm signal from high redshifts ( $z > 500$ ) at low observed frequencies ( $\nu < 2.84$  MHz). Since the color temperature, and hence the spin temperature at these redshifts, changes its behavior relatively to  $T_{CMB}$  with redshift (as shown in Figure 2), the signal is expected to be seen in emission at  $640 \lesssim z \lesssim 850$  and in absorption

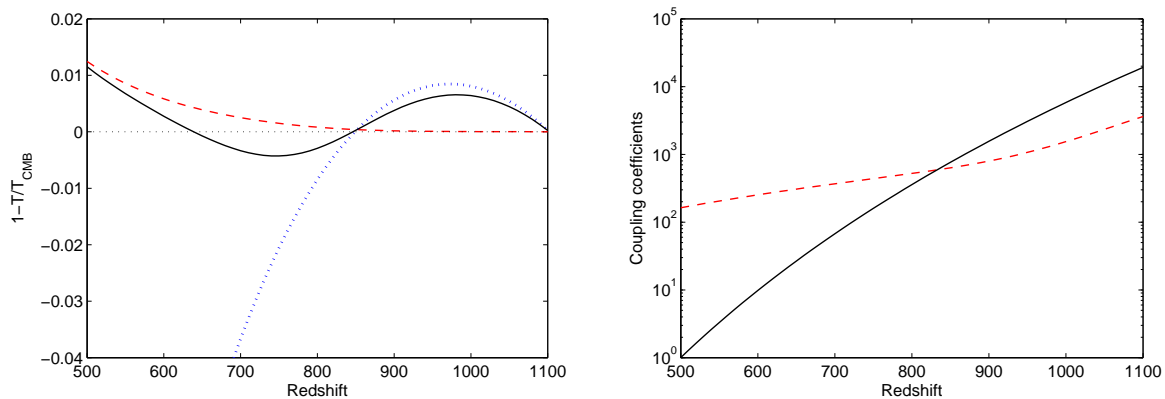


**Figure 2.** *Left:* Reshift evolution for the fractional contrast factors of various temperatures  $T_i$  relative to the CMB temperature,  $(1 - T_i/T_{CMB})$ . We show the kinetic gas temperature  $T_i = T_K$  (red dashed), spin temperature  $T_i = T_S$  (black solid) and color temperature  $T_i = T_C$  (blue dotted). *Right:* Coupling coefficients as a function of redshift. We show the Wouthuysen-Field coupling coefficient (black solid curve) and the collisional coupling including H-H, H-p and H-e collisions (red dashed curve). The Wouthuysen-Field effect becomes dominant at  $z \gtrsim 850$ .

at  $850 \lesssim z \lesssim 1100$ . The amplitude of the emission signal peaks at  $z \sim 750$  where it reaches a value of  $T_b = 0.9$  mK, instead of  $-0.35$  mK in the collisions-only case previously considered in the literature. The minimum of the absorption signal during the recombination era is reached at  $z \sim 980$  with a value of  $T_b = -1.5$  mK instead of  $-0.01$  mK in the collisions-only case. Note that since the intensity of the radiation field around Ly $\alpha$  resonance is well defined by atomic physics (calculated here through the CosmoRec code), one should be able to predict the signal precisely for a fixed set of cosmological parameters.

Despite the growing intensity of Ly $\alpha$  photons towards higher redshifts (as shown on Figure 1), the 21-cm signal from  $z > 1060$  diminishes, since the optical depth for free-free absorption of 21-cm photons exceeds unity. This defines a fundamental cutoff in redshift space beyond which the 21-cm signal cannot be observed. Note that the Thompson optical depth of redshifted 21-cm signal is smaller than 10% at all redshifts of interest, implying that observations of the 21-cm signal at redshifts below the cutoff (and above the redshift of reionization) are in principle possible.

Next, we consider the effect of the early Ly $\alpha$  photons on the power spectrum of the 21-cm signal. The WF effect is essential in maintaining the 21-cm signal at high redshifts, as shown by the right panel of Figure 3. During and after recombination but before formation of first stars, the main source of fluctuations is perturbations in the neutral hydrogen density,  $\delta n_{HI}/n_{HI}$  [18]. Since the ionization fraction during recombination is expected to be nearly uniform, this quantity follows the baryon density perturbations  $\delta_b \equiv (\delta \rho_b/\rho_b)$ , which we here find using the online version of the CAMB code [32]. Ignoring other sources of fluctuations, the wavenumber dependence of the 21-cm power spectrum is that of the baryonic density field, with the early



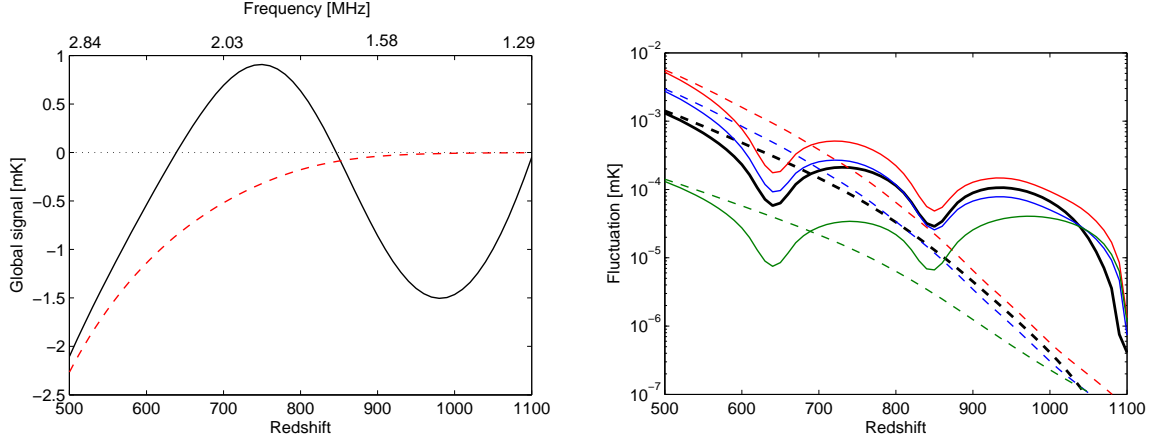


**Figure 3.** *Left:* The amplitude of 21-cm brightness temperature in mK when accounting only for collisions (dashed, red) and when adding the effect of the Ly $\alpha$  photons (solid black). The Ly $\alpha$  contribution is noticeable at  $z > 500$ . *Right:* The fluctuations in the 21-cm background in mK (defined via Eq. 2.4) versus redshift including the WF coupling  $x_\alpha$  (solid curves) and ignoring it (dashed curves) for comoving wavenumbers  $k = 5 \text{ Mpc}^{-1}$  (red),  $k = 0.5 \text{ Mpc}^{-1}$  (blue), the Baryonic Acoustic Oscillations (BAO) scale  $k = 0.05 \text{ Mpc}^{-1}$  (boldface, black), and  $k = 5 \text{ Mpc}^{-1}$  (green).

WF coupling affecting its redshift-dependent amplitude. In this regime, perturbations in  $T_b$  trace perturbations in hydrogen density  $\delta T_b = \frac{dT_b}{dn_{HI}} \delta n_{HI}$ , and we can analytically derive the fluctuations in the 21-cm field to be,

$$\delta T_b = T_b \sqrt{1.87} \left[ \frac{2 + x_\alpha + x_c}{1 + x_\alpha + x_c} \right] \delta_b, \quad (2.4)$$

where we accounted for the dependence of  $\tau$ ,  $x_c$  and  $x_\alpha$  on  $n_H$ . The factor  $\sqrt{1.87}$  accounts for the spherically-averaged contribution of peculiar velocities to the fluctuation amplitude of the brightness temperature within linear theory [33]. (In the case when the WF coupling is ignored, this equation becomes  $\delta T_b = T_b \sqrt{1.87} \left[ \frac{2+x_c}{1+x_c} \right] \delta_b$ .) The right frame of Figure 3 shows the redshift dependence of the 21-cm fluctuations at particular comoving wavenumbers for the two cases: with and without the early Ly $\alpha$  background assuming a standard set of cosmological parameters [26]. In general, fluctuations from redshifts  $z > 500$  are very small compared to the gravitationally-amplified fluctuations at lower redshifts (for example, the maximal fluctuation from collisions reach the  $\sim 0.6 \text{ mK}$  level at the BAO wavenumber scale at  $z \sim 50$ ), mainly due to the smallness of the density perturbations in baryons at  $z \sim 10^3$  whose growth was suppressed by the CMB before recombination. However Ly $\alpha$  photons prevent the 21-cm signal at high redshifts from decaying and keep it at a nearly constant amplitude of  $\mathcal{O}(10^{-5} - 10^{-4}) \text{ mK}$ , while the previously calculated (collisions-only) amplitude decays exponentially fast with increasing redshift. The ratio of the two signals is scale independent and peaks at  $z \sim 1060$  (the redshift after which the 21-cm signal drops due to free-free absorption) where it reaches a value of 230, with a secondary peak in the ratio obtained at a lower redshift  $z \sim 790$  with a value of 3.5.



### 3 Conclusions

We performed the first calculation of the effect of the Ly $\alpha$  radiation background during the epoch of recombination on the 21-cm signal from cosmic hydrogen. We found that the Wouthuysen-Field coupling of the 21-cm signal to the color temperature of the Ly $\alpha$  radiation elevates the global 21-cm signal at observed frequencies  $\nu < 2.84$  MHz (or wavelengths  $\lambda > 100$  meters), to a milli-Kelvin level in the redshift range  $z \sim 500 - 1100$ . The power spectrum of 21-cm brightness fluctuations obtains an amplitude of order  $(10^{-5}-10^{-4})$  mK, well above previous predictions which ignored the Ly $\alpha$  background. At redshifts higher than  $z \sim 1060$  ( $\nu < 1.34$  [MHz] or  $\lambda > 222$  meters) the cosmic plasma becomes opaque to the 21-cm signal due to free-free absorption.

Even though the Ly $\alpha$  coupling greatly increases the expected 21-cm signal from the hydrogen recombination epoch, detection of the hectometer waves, which must be done from space with a lunar or a free-flying antenna array, still appears very futuristic. However, ongoing interest in the ultra-long wavelength regime which was largely unexplored so far, as well as technological advances in instrumentation, might eventually lead to the construction of related observatories and possibly even to the detection of the global 21-cm signal in the 1.5–3 MHz band. To access the cosmic signal, a thorough study of the Galactic emission at the very low frequencies must be conducted. The first observations in the frequency range of 0.4–6.5 MHz were done in the 1970s by the Radio Astronomy Explorer satellite [12]. The spectrum measured by this satellite was dominated by the Galactic absorption and emission and reached the maximal brightness temperature of  $\sim 4 \times 10^9$  mK at 3 MHz, which is nine orders of magnitude stronger than the cosmic signal predicted here. This result was later confirmed by measurements of the spectrum at 0.2–13.8 MHz by the WAVES instrument on the WIND spacecraft [14]. Hopefully, the technology developed at present for the reconstruction of the 21-cm signal from lower redshifts, where the Galactic emission is “only”  $\sim 10^5$  stronger than the cosmic signal, will pave the way to the detection of the 21-cm from recombination. Proposals for radio astronomy on the moon [16] suggest observations in the frequency range 1–10 MHz as one of their primary goals. As a first step, it is being suggested to install a single lunar antenna operating in the frequency range of 1 kHz–100 MHz, which could serve as a pathfinder for a future lunar array to detect the 21-cm signal from high redshifts. One of the goals of such an array would be to map the signal at frequencies inaccessible from the ground which are completely reflected by the ionosphere of the Earth, i.e. 1–10 MHz, matching the range of frequencies that define the 21-cm signal from recombination. The other band of interest is 10–100 MHz, where the incoming phase of the radiation is distorted by the ionosphere. Currently, there exists an unfunded ESA proposal to launch a Lunar Lander with such a path-finder antenna on board. Another proposed project involves the construction of a radio observatory on the lunar surface [17]. Although its primary goal concerns imaging of the radio emission generated by solar bursts at frequencies below 10 MHz and studying the lunar ionosphere, the proposed observatory is also designed to serve as a path-finder for a larger array on the moon focused on cosmology.

If observed, the 21-cm signal from  $z > 500$  will provide a unique, independent and rich probe of the early Universe. For a fixed set of cosmological parameters and no new physics, the expected signal depends solely on atomic physics and is not “contaminated” by the products of star formation. Therefore, it offers a unique three-dimensional probe (as opposed to the

CMB which probes only the two-dimensional surface of last scatter) of cosmological parameters and primordial density perturbations, allowing refined tests of the  $\Lambda$ CDM model, the properties of the dark matter and dark energy, as well as theories of modified gravity and inflationary cosmology. Since the 21-cm signal does not suffer from Silk damping on small scales, it allows to set new constraints on the spectrum of isocurvature perturbations on extremely small scales (down to the Jeans length [18]) where a blue tilt [34] would be manifested.

Our study was made possible by recent advances in the theory of recombination, encapsulated by the codes CosmoRec and HyRec which calculate the radiative transfer of the Ly $\alpha$  line. We found order unity differences between the predictions for the 21-cm signal from the two available codes, and hence conclude that a better treatment of the Ly $\alpha$  background is needed in order to reach the level of precision characterizing the current standard for predictions of CMB anisotropies.

## Acknowledgments

We thank Y. Ali-Haimoud and J. Chluba for useful discussions about the HyRec and CosmoRec codes. This work was sponsored by the Raymond and Beverly Sackler Tel-Aviv University Harvard/ITC Astronomy Program, additional support was obtained from Israel Science Foundation grant 823/09, the LabEx ENS-ICFP: ANR-10-LABX-0010/ANR-10-IDEX-0001-02 PSL and NSF grant AST-1312034.

## References

- [1] Loeb, A., Furlanetto, S., *The First Galaxies in the Universe* Princeton University Press (2012).
- [2] Pritchard, J. R., Loeb, *21 cm cosmology in the 21st century RPP* **75** (2012) 6901.
- [3] Furlanetto, S. R., Oh, S. P., Briggs, F. H., *Cosmology at low frequencies: The 21 cm transition and the high-redshift Universe, PhR* **433** (2006) 181.
- [4] Bowman J. D., Morales M. F., Hewitt J. N., *Foreground Contamination in Interferometric Measurements of the Redshifted 21 cm Power Spectrum ApJ* **695** (2009) 183.
- [5] Harker, G., *Power spectrum extraction for redshifted 21-cm Epoch of Reionization experiments: the LOFAR case MNRAS* **405** (2010) 2492.
- [6] Parsons, A., R., Liu, A., Aguirre, J. E., Ali, Z. S., Bradley, R. F., *New Limits on 21cm EoR From PAPER-32 Consistent with an X-Ray Heated IGM at z=7.7, arXiv:1304.4991* (2013).
- [7] Greenhill, L. J., Bernardi, G., *HI Epoch of Reionization Arrays, arXiv:1201.1700* (2012).
- [8] Mellema G., Koopmans, L. , Abdalla, F., Bernardi, G., Ciardi, B., *Reionization and the Cosmic Dawn with the Square Kilometre Array ExA* **36** (2013) 235.
- [9] Burns, J. O., Lazio, J., Bale, S., Bowman, J., Bradley, R., et. al., *Probing the first stars and black holes in the early Universe with the Dark Ages Radio Explorer (DARE) AdSpR* **49** (2012) 433.
- [10] Cane, H. V., Whitham, P. S., *Observations of the southern sky at five frequencies in the range 2-20 MHz MNRAS* **179** (1977) 21; Ellis, G. R. A., Mendillo, M., *A 1.6 MHz survey of the galactic background radio emission Australian Journal of Physics* **40** (1978), 705; Cane, H. V., Erickson, W. C., *A 10 MHz map of the galaxy Radio Science* **36** (2001) 1765.

- [11] Novaco, J. C., Brown, L. W., *Nonthermal galactic emission below 10 megahertz* *ApJ* **221** (1978) 114.
- [12] Alexander, J. K., Brown, L. W., Clark, T. A., Stone R. G., Weber, R. R., *The Spectrum of the Cosmic Radio Background Between 0.4 and 6.5 MHz* *ApJ* **157** (1969) 163.
- [13] Brown L. W., *The Galactic radio spectrum between 130 and 2600 kHz* *ApJ* **180** (1973) 359.
- [14] Manning R., Dulk, G. A., *The Galactic background radiation from 0.2 to 13.8 MHz* *A&A* **372** (2001) 663.
- [15] Weiler, K. W., Johnston, K. J., Simon, R. S., Dennison, B. K., Erickson, W. C., Kaiser, M. L., Cane, H. V., Desch, M. D., *A low frequency radio array for space* *A&A* **195** (1988) 372.
- [16] Wolt M., K., Aminaei, A., Zarka, P., Schrader, J., Boonstra, A., Falcke, H., *Radio astronomy with the European Lunar Lander: Opening up the last unexplored frequency regime* *P&SS* **74** (2012) 167.
- [17] Lazio, T. J. W., MacDowall, R. J., Burns, J. O., Jones, D. L., Weiler, K. W., Demaio, L., Cohen, A., Paravastu D. N., Polisensky, E., Stewart, K., Bale, S., Gopalswamy, N., Kaiser, M., Kasper, J., *The Radio Observatory on the Lunar Surface for Solar studies* *ASR* **48** (2011) 1942.
- [18] Loeb, A., Zaldarriaga, M., *Measuring the Small-Scale Power Spectrum of Cosmic Density Fluctuations through 21cm Tomography Prior to the Epoch of Structure Formation*, *PRL* **92** (2004) 3520.
- [19] Lewis, A., Challinor, A., *21cm angular-power spectrum from the dark ages*, *PhRvD* **76** (2007) 3005.
- [20] Wouthuysen, S. A., *On the excitation mechanism of the 21-cm (radio-frequency) interstellar hydrogen emission line*, *AJ* **57** (1952) 31.
- [21] Field, G. B., *Excitation of the Hydrogen 21-CM Line*, *Proc. Institute Radio Energeers* **46** (1958) 240.
- [22] Ali-Haimoud, Y., Hirata, C. M., *HyRec: A fast and highly accurate primordial hydrogen and helium recombination code*, *Phys. Rev. D* **83** (2011) 043513.
- [23] Chluba, J., Thomas, R. M., *Towards a complete treatment of the cosmological recombination problem*, *MNRAS* **412** (2011) 748.
- [24] Ali-Haimoud, Y., Hirata, C. M., *Ultrafast effective multilevel atom method for primordial hydrogen recombination*, *Phys. Rev. D* **82** (2010) 063521.
- [25] Chluba, J., Sunyaev, R. A., *Cosmological recombination: feedback of helium photons and its effect on the recombination spectrum*, *MNRAS* **402** (2010) 1221.
- [26] Planck Collaboration; Ade, P. A. R., Aghanim, N., Armitage-Caplan, C., Arnaud, M., Ashdown, M., et al., *Planck 2013 results. XVI. Cosmological parameters* arxiv:1303.5076.
- [27] Hirata C. M., Forbes, J., *Lyman- $\alpha$  transfer in primordial hydrogen recombination* *PRD* **80** (2009) 3001.
- [28] Fialkov A., Barkana R., Tseliakhovich D., Hirata C. M., *Impact of the relative motion between the dark matter and baryons on the first stars: semi-analytical modelling* *MNRAS* **424** (2012) 1335; Naoz, S., Noter, S., Barkana R., *The first stars in the Universe* *MNRAS* **3734** (2006) 98.
- [29] Furlanetto, S. R., Furlanetto, M. R., *Spin-exchange rates in electronhydrogen collisions*, *MNRAS* **374** (2007) 547.
- [30] Furlanetto, S. R., Furlanetto, M. R., *Spin-exchange rates in protonhydrogen collisions*, *MNRAS* **379** (2007) 130.

- [31] Peebles, P. J. E., *Recombination of the Primeval Plasma*, *ApJ* **153** (1968) 1.
- [32] Lewis A., Bridle, S., *Cosmological parameters from CMB and other data: a Monte- Carlo approach* *PRD* **66** (2002) 103511.
- [33] Barkana, R., Loeb A., *A Method for Separating the Physics from the Astrophysics of High-Redshift 21 Centimeter Fluctuations* *ApJ* **624** (2005) 65.
- [34] Sollom, I., Challinor, A., Hobson, M.P., *Cold dark matter isocurvature perturbations: Constraints and model selection*, *PRD* **79** (2009) 123521; Beltran, M., Garcia-Bellido, J., Lesgourgues, J., Riazuelo, A., *Bounds on cold dark matter and neutrino isocurvature perturbations from CMB and LSS data*, *PRD* **70** (2004) 103530; Beltran, M., Garcia-Bellido, J., Lesgourgues, Viel, M., ., *Squeezing the window on isocurvature modes with the Lyman- $\alpha$  forest*, *PRD* **72** (2005) 103515; Valiviita, J., Giannantonio, T., *Constraints on primordial isocurvature perturbations and spatial curvature by Bayesian model selection*, *PRD* **80** (2009) 123516.